

# SECONDARY ELECTRON EMISSION COEFFICIENTS FOR PROBE DIAGNOSTICS AT ATMOSPHERIC PRESSURE PLASMA

M. RASHIT TALUKDER

RECEIVED : 15th July, 2005

*Effective secondary electron emission coefficients have been estimated using a kinetic model for tungsten-noble gas combinations for a wide range of energies of the emitted secondary electrons and  $E/p$  factors. Algebraic equations are derived, using the estimated secondary electron emission coefficients and presented in a suitable form in order to calculate the secondary electron emission current from the probe due to the interactions of metastable atoms and metal probe, and can be directly applied for probe data simulation.*

**INTRODUCTION :** High pressure nonthermal plasmas are drawing much attraction for reactive plasma processing. For such plasma source design and discharge performance optimization, appropriate information regarding plasma parameters and their spatiotemporal behaviours are required [1]. The Langmuir probe is a widely used diagnostic tool to determine the plasma parameters because it can provide local plasma properties, which are difficult to determine by other diagnostic techniques [2]. It is known that the secondary electron emission from the metal probe is a parasitic effect for probe diagnostic. Secondary electrons can be emitted from the metal surface [3–6] due to the interactions of electrons, ions, metastable atoms, and photons. Negative ions [7], charged [8] particles, and dust [9] particles, are produced due also to their interactions and can change the probe characteristics measured in plasma. The emitted electrons from the probe can lead to erroneous measurements [10] of ion and electron currents either at negative or positive probe potentials. So it is very important to take into considerations the existence and the effects of the above mentioned charged particles in plasma during the measurements of probe characteristics. The effective secondary electron emission coefficient (ESEC) has been estimated for tungsten-noble gas combination and hence presented, in this report, in a suitable form that can easily be used for the analyses of probe data measured in atmospheric pressure plasma.

**THEORY :** The effective secondary electron emission coefficient (ESEC)  $\gamma$  is defined by the number of electrons leaving the emitting surface per impinging primary particles. In high pressure high density gases,  $\gamma$  increases with the increase of  $E/p$  at lower values but becomes saturated [11] at higher  $E/p$  values, where  $E$  is the electric field and  $p$  is the gas pressure. The mechanism of this dependence can be described due to the reflection of a part of the secondary electrons from the gas atoms back to the metal surface because of high gas density. A qualitative expression describing such behaviour, has been proposed using J.J. Thompson's simple hydrodynamic model, is given [12] by

$$\frac{\gamma}{\gamma_0} = \frac{4v_d}{(\bar{v}_0 + 4v_d)}, \quad \dots (1)$$

where  $\gamma_0$  is secondary emission coefficient in vacuum,  $\bar{v}_0$  is average velocity of the emitted electrons, and  $v_d$  is the drift velocity of electrons.

A kinetic approach has been adopted [13], assuming that the mean free path  $\lambda_e$  of electrons is much less than the scale length  $L$ , the electric field  $E$  is weak such that  $eE\lambda_e \ll \epsilon_k$ , where  $\epsilon_k$  is the kinetic energy of electron, the electric field is uniform, assumed for simplicity, and neglecting the energy exchange between collisions of electrons and heavy particles, and the excitation and ionization energies of the particles are much higher than the emitted secondary electrons near the metal surface. The maximum energy of the emitted electrons [14, 15] is given by  $\epsilon_{i, \max} = \epsilon_i - 2\phi$  for ions and  $\epsilon_{ex, \max} = \epsilon_{ex} - \phi$  for metastable atoms, where  $\epsilon_i$  and  $\epsilon_{ex}$  are the ionization and excitation energies, respectively and  $\phi$  is the work function of the material. Because of high pressure, the electric field will be reduced and the mean free path of electron will be small compared to the scale length. Consequently the kinetic energy of the electrons gained from the electric field will be less between two collisions. Assuming the isotropic electron velocity distribution function, ESEC can be written [13] as

$$\gamma\left(\epsilon_0, \frac{E}{p}\right) = \frac{f(\epsilon_0) \gamma_0}{1 + \frac{3\epsilon_0}{4\epsilon_{ex}} \left(\frac{\sigma_m(\epsilon_{ex})}{\sigma'_i(\epsilon_{ex}) eE\lambda_e}\right)^{1/3} + \frac{3}{4\nu_0} \int_0^z \frac{\nu_i(z) dz}{(1 + eEz/\epsilon_0)^{3/2}}} \quad \dots (2)$$

where  $f(\epsilon_0) \gamma_0$  is the differential secondary electron emission coefficient in vacuum,  $z$  is the length where no inelastic collision takes place and assuming that  $L \gg z$ , and  $f(\epsilon_0)$  is a function that represents the emitted electrons having initial energies in the range from  $\epsilon_0$  to  $\epsilon_0 + d\epsilon_0$ , satisfying the normalized condition

$$\int_0^{\epsilon_{ex}} f(\epsilon_0) d\epsilon_0 = 1, \quad \dots (3)$$

$\sigma_m$  is the momentum transfer cross section,  $\nu_i$  is the frequency at excitation threshold  $\epsilon_{ex}$ ,  $\sigma'_i$  is the energy derivative of collision cross section at ionization threshold  $\epsilon_i$ . Now integrating Eq. (2) over the kinetic energy of the electron from  $\epsilon_0$  to  $\epsilon_0 + eEz$ , we obtain

$$\frac{\gamma(\epsilon_0, E/p)}{\gamma_0} = \frac{f(\epsilon_0)}{1 + \frac{3\epsilon_0}{3\epsilon_{ex}} \left(\frac{\sigma_m(\epsilon_{ex})}{\sigma'_i(\epsilon_{ex}) eE\lambda_e}\right)^{1/3} + \frac{3n_g \epsilon_0}{4eE} \int_{\epsilon_0}^{\epsilon_{ex}} \frac{\sigma_m(\epsilon) d\epsilon}{\epsilon}} \quad \dots (4)$$

Eq. (4) can be rewritten in a more convenient form as

$$\frac{\gamma(\epsilon, E/p)}{\gamma_0} = \frac{f(\epsilon_0)}{1 + \epsilon_n \alpha \left(\frac{\bar{\chi}}{\chi}\right)^{1/3} + \psi(\epsilon_n) \left(\frac{\bar{\chi}}{\chi}\right)}, \quad \dots (5)$$

where  $\epsilon_n = \frac{\epsilon_0}{\epsilon_{ex}}$ , and  $\chi$  is the reduced magnitude of the electric field given by

$$\chi \equiv \frac{E}{p}, \quad \dots (6)$$

the characteristic electric field  $\bar{\chi}$  reduced to a pressure of 1 Torr can be represented as

$$\bar{\chi} = \frac{E}{p} = \frac{\epsilon_{ex}}{e\lambda_e \kappa T_n n_g} = \frac{\epsilon_{ex}}{e} \cdot \frac{\sigma_m(\epsilon_{ex})}{\kappa T_n}, \quad \dots (7)$$

where  $\kappa$  is the Boltzmann constant,  $n_g$  is the neutral particle concentration at temperature  $T_n$  and  $e$  is the electronic charge. The normalized energy dependent function  $\psi(\epsilon_n)$  and the coefficient  $\alpha$  are given by

$$\psi(\epsilon_n) = \frac{3\epsilon_n}{4} \int_{\epsilon_n}^1 \frac{\sigma_m(\epsilon_{ex}y) dy}{\sigma_m(\epsilon_{ex})y}, \quad \dots (8)$$

$$\alpha = \frac{3}{4} \left[ \frac{\sigma_m(\epsilon_{ex})}{\sigma_m'(\epsilon_{ex})\epsilon_{ex}} \right]^{1/3}, \quad \dots (9)$$

Eq. (8) has been solved numerically and approximated by the following empirical equation in order to use it for simulation for Langmuir probe data analyses as

$$\psi(\epsilon_n) \approx C \frac{\epsilon_n(1-\epsilon_n)}{1 + D\epsilon_n}, \quad \dots (10)$$

where the constants  $C$  and  $D$  depend on the gas-material combination [13].

The resulting ESEC can be obtained as a function of the electric field by integrating Eq. (5) over the energy range from 0 to  $\epsilon_m$  as

$$\gamma(\epsilon, \chi) = \int_0^{\epsilon_m} \gamma(\epsilon_0, \chi) d\epsilon_0, \quad \dots (11)$$

where  $\epsilon_m$  is the maximum energy of the emitted electrons. Eqs. (5) and (11) have been used to determine ESEC of tungsten for helium- and xenon-like gases. For helium-like gases, it has been assumed that the energy distribution of the emitted electrons are wide and most of them have energies where the function  $\psi(\epsilon_n)$  has a maximum and there are no major changes over the energy range [14]. In case of xenon-like gases, when all the emitted secondary electrons have energies in the lower energy range such that the maximum energy  $\epsilon_m$  of the secondary electrons is less than the energy at which the function  $\psi(\epsilon_n)$  has its maximum.

**(1) Helium-like gases :** The average value  $\bar{\psi}_{He}(\bar{\epsilon}_m)$  of the function  $\psi(\epsilon_n)$  can be obtained by integrating the function  $\psi(\epsilon_n)$  over the energy range from 0 to  $\bar{\epsilon}_m$

$$\bar{\psi}_{He}(\bar{\epsilon}_m) = \int_0^{\bar{\epsilon}_m} \psi(\epsilon_n) f(\epsilon_{ex}\epsilon_n) \epsilon_{ex} d\epsilon_n, \quad \dots (12)$$

where  $\bar{\epsilon}_m = \epsilon_m/\epsilon_{ex}$ , and integrating Eq. (5) one can write ESEC as

$$\frac{\bar{\gamma}(\bar{\epsilon}_m, \chi)}{\gamma_0} = \frac{1}{\alpha\bar{\epsilon}_m} \left( \frac{\chi^0}{\bar{\chi}} \right)^{1/3} \ln \left[ \frac{1 + \bar{\psi}_{He}(\bar{\epsilon}_m) \bar{\chi}/\chi + \alpha\bar{\epsilon}_m (\bar{\chi}/\chi)^{1/3}}{1 + \bar{\psi}_{He}(\bar{\epsilon}_m) \bar{\chi}/\chi} \right] \quad \dots (13)$$

Estimations have been done using Eq. (13) for helium shown, as a reference, by marks in Fig. 1 for 100, 400 and 700 Torr. Algebraic equation for  $\bar{\gamma}(\bar{\epsilon}_m, \chi)/\gamma_0$  best fitted to the data estimated using Eq. (13) is deduced by linear function. Dependence of  $\bar{\gamma}(\bar{\epsilon}_m, \chi)/\gamma_0$  on  $\chi$ .  $\bar{\gamma}(\bar{\epsilon}_m, \chi)/\gamma_0$  is empirically presumed as

$$\frac{\bar{\gamma}(\bar{\epsilon}_m, \chi)}{\gamma_0} = A(\bar{\epsilon}_m, \chi) + B(\bar{\epsilon}_m, \chi) \chi. \quad \dots (14)$$

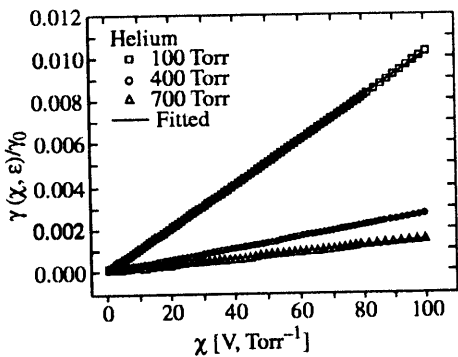


Fig. 1. Estimation and fitting of ESEC for  $\epsilon_m = 1$  eV in He.

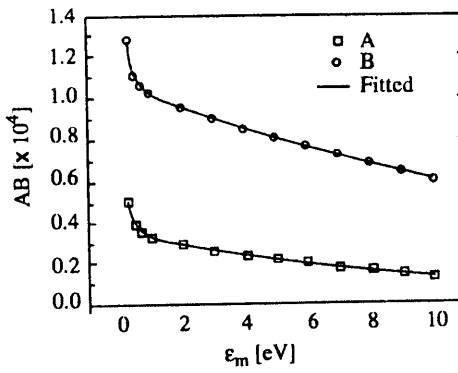


Fig. 2. Fitting for  $A$  and  $B$  as a function of  $\epsilon_m$  for  $p = 100$  Torr.

Figure 1 shows that the solid curves calculated by Eq. (14) fit well with the estimated ESEC data using Eq. (13) for each  $\epsilon_m$  by adjusting the values of  $A$  and  $B$  for the specific pressure. Dependence of  $A$  and  $B$  on  $\chi$  for 100, 400, and 700 Torr for the selected values of  $\epsilon_m$  have been included in Table 1 for reference. However, at the present situation, the values of  $A$  and  $B$  can be applied for the specific values of  $\epsilon_m$  given in Table 1. For the use in the Langmuir probe data simulation, the values of  $A$  and  $B$  should be given not only as a function of  $\chi$  but also for any value of  $\epsilon_m$ . Hence  $A$  and  $B$  can be approximated by the following exponential function of  $\epsilon_m$  for helium, respectively, as

$$A = A_0 + A_1 \exp\left(\frac{-\epsilon_m}{0.17}\right) + A_2 \exp\left(\frac{-\epsilon_m}{8.80}\right), \quad \dots (15)$$

$$B = B_0 + B_1 \exp\left(\frac{-\epsilon_m}{0.17}\right) + B_2 \exp\left(\frac{-\epsilon_m}{15.80}\right). \quad \dots (16)$$

Table 1 : Dependence of  $A$  and  $B$  on  $\epsilon_m$  for He-W (e.g., 5.06E-5 indicates  $5.06 \times 10^{-5}$ )

$T_e$ [eV]	100 Torr		400 Torr		700 Torr	
	$A (\epsilon_m)$	$B (\epsilon_m)$	$A (\epsilon_m)$	$B (\epsilon_m)$	$A (\epsilon_m)$	$B (\epsilon_m)$
0.3	5.06E-5	1.28E-4	2.51E-4	3.09E-4	1.68E-6	1.88E-5
0.5	3.90E-5	1.12E-4	1.94E-4	2.70E-4	1.30E-6	1.63E-5
0.7	3.56E-5	1.06E-4	1.77E-4	2.57E-4	1.18E-6	1.55E-5
1.0	3.29E-5	1.02E-4	1.64E-4	2.49E-4	1.09E-6	1.50E-5
2.0	2.91E-5	9.55E-5	1.46E-4	2.32E-4	9.67E-7	1.39E-5
3.0	2.63E-5	9.02E-5	1.31E-4	2.19E-4	8.73E-7	1.32E-5
4.0	2.38E-5	8.53E-5	1.19E-4	2.08E-4	7.91E-7	1.24E-5
5.0	2.15E-5	8.06E-5	1.07E-4	1.97E-4	7.16E-7	1.17E-5
6.0	1.94E-5	7.62E-5	9.71E-5	1.86E-4	6.48E-7	1.11E-5
7.0	1.75E-5	7.20E-5	8.78E-5	1.76E-4	5.86E-7	1.05E-5
8.0	1.58E-5	6.80E-5	7.92E-5	1.66E-4	5.30E-7	9.87E-6
9.0	1.43E-5	6.42E-5	7.14E-5	1.57E-4	4.78E-7	9.31E-6
10.0	1.29E-5	6.07E-5	6.46E-5	1.49E-4	4.34E-7	8.80E-6

For reference, the fitted curves for  $A$  and  $B$  are shown in Fig. 2 for 100 Torr in helium. Using Eq. (14) along with Eqs. (15) by introducing the pressure dependence coefficients of  $A$  and  $B$  from Table II, one can easily fit  $\bar{\gamma}(\bar{\epsilon}_m, \chi)/\gamma_0$  to any  $\epsilon_m$  from 0.3 to 10 eV.

**Table 2 : Dependence of  $A$  and  $B$  on  $p$  for He-W.**

$p$ [Torr]	$A_0$	$A_1$	$A_2$	$B_0$	$B_1$	$B_2$
100	1.93E-6	9.00E-5	3.00E-5	7.07E-6	1.30E-4	1.02E-4
200	5.90E-7	3.00E-5	1.00E-5	3.28E-6	7.00E-5	5.11E-5
300	2.98E-7	1.00E-5	4.98E-6	2.12E-6	4.00E-5	3.46E-5
400	1.84E-7	7.96E-6	3.01E-6	1.56E-6	3.00E-5	2.61E-5
500	1.27E-7	5.40E-6	2.04E-6	1.24E-6	3.00E-5	2.08E-5
600	9.35E-8	3.93E-6	1.48E-6	1.02E-6	2.00E-5	1.74E-5
700	7.24E-8	3.00E-6	1.13E-6	1.58E-6	2.00E-5	1.39E-5

Similar to the derivation of Eq. (14) and Eqs. (15), the estimated values of ESEC have been fitted using Eq. (14) by adjusting the values of  $A$  and  $B$  for the pressure ranges from 100 to 700 Torr for neon. Now the values of  $A$  and  $B$  have been approximated by the following exponential functions of  $\epsilon_m$  for neon, respectively, as

$$A = A_0 + A_1 \exp\left(\frac{-\epsilon_m}{0.1858}\right) + A_2 \exp\left(\frac{-\epsilon_m}{4.038}\right), \quad \dots (16a)$$

$$B = B_0 + B_1 \exp\left(\frac{-\epsilon_m}{0.2196}\right) + B_2 \exp\left(\frac{-\epsilon_m}{5.475}\right). \quad \dots (16b)$$

For reference, the estimated values given by marks and the fitted curves given by continuous line are shown in Fig. 3 for  $\epsilon_m = 1$  eV of the emitted electrons in neon. Now using Eq. (14) along with Eqs. (16) by introducing the pressure dependence coefficients of  $A$  and  $B$  from Table III, one can easily fit  $\bar{\gamma}(\bar{\epsilon}_m, \chi)/\gamma_0$  to any  $\epsilon_m$  from 0.3 to 10 eV.

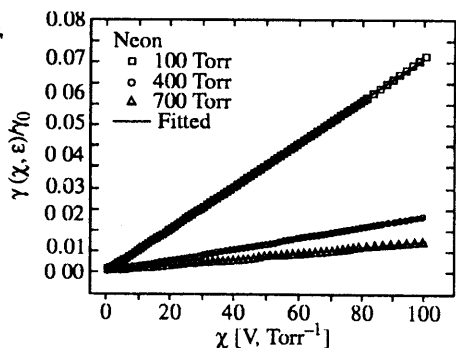


**Fig. 3. Estimation and fitting of ESEC for  $\epsilon_m = 1$  eV in Ne.**

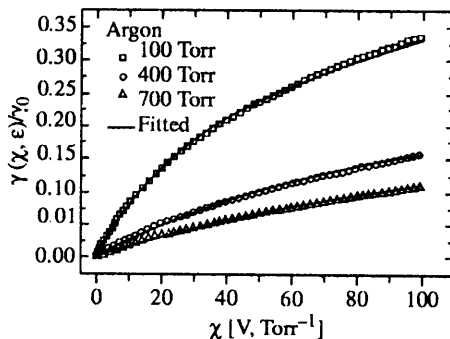


**Fig. 4. Estimation and fitting of ESEC for  $\epsilon_m = 1$  eV in Ar.**

Table 3 : Coefficients of A and B for Ne-W.

$p$ [Torr]	$A_0$	$A_1$	$A_2$	$B_0$	$B_1$	$B_2$
100	4.20E-4	2.31E-3	8.30E-4	4.70E-4	7.00E-4	3.90E-4
200	1.30E-4	1.08E-3	2.40E-4	2.40E-4	5.20E-4	2.00E-4
300	6.00E-5	5.40E-4	1.20E-4	1.70E-4	3.60E-4	1.40E-4
400	4.00E-5	4.80E-4	7.00E-5	1.30E-4	3.80E-4	1.00E-4
500	3.00E-5	2.20E-4	5.00E-5	1.00E-4	2.30E-4	9.00E-5
600	2.00E-5	1.60E-4	3.00E-5	8.00E-5	1.90E-4	7.00E-5
700	1.00E-5	1.20E-4	3.00E-5	7.00E-5	1.70E-4	6.00E-5

(2) **Xenon-like gases** : In this case the average value  $\bar{\Psi}_{Xe}(\bar{\epsilon}_m)$  of the function  $\Psi(\epsilon_n)$  can be approximated by a linear function reads as

$$\bar{\Psi}_{Xe}(\bar{\epsilon}_m) = \epsilon_n \Psi(\bar{\epsilon}_m)/\bar{\epsilon}_m. \quad \dots (17)$$

and by integrating Eq. (5) over the energy range from 0 to  $\bar{\epsilon}_m$ , ESEC can be obtained as

$$\bar{\gamma}(\bar{\epsilon}_m, \chi)/\gamma_0 = \ln(1 + \beta\bar{\epsilon}_m)/\beta\bar{\epsilon}_m, \quad \dots (18)$$

where

$$\beta = \bar{\Psi}_{Xe}(\bar{\epsilon}_m) \bar{\chi}/\chi\bar{\epsilon}_m (\bar{\chi}/\chi)^{1/3}. \quad \dots (19)$$

In the way similar to helium-like cases, estimation have been done using Eq. (19) for argon, krypton and xenon shown by marks in Figs. 4, 5, and 6 respectively. Algebraic equation for  $\bar{\gamma}(\bar{\epsilon}_m, \chi)/\gamma_0$  best fitted to the data estimated using Eq. (19) is deduced by a hyperbolic function. After somewhat tedious considerations concerned with the dependence of  $\bar{\gamma}(\bar{\epsilon}_m, \chi)/\gamma_0$  on  $\chi$ ,  $\bar{\gamma}(\bar{\epsilon}_m, \chi)/\gamma_0$  is empirically presumed as

$$\bar{\gamma}(\bar{\epsilon}_m, \chi)/\gamma_0 = 1 - \{1 + A(\bar{\epsilon}_m, \chi) \cdot (\chi)\}^{-1/B(\bar{\epsilon}_m, \chi)}. \quad \dots (20)$$

Similarly, the estimated values of ESEC have been fitted using Eq. (20) by adjusting the values of  $A$  and  $B$  for the pressure ranges from 100 to 700 Torr for argon, krypton and xenon, respectively. Now  $A$  and  $B$  can be approximated by the following exponential functions of  $\epsilon_m$ , respectively, for argon as

$$A = A_0 + A_1 \exp\left(\frac{-\epsilon_m}{1.717}\right) + A_2 \exp\left(\frac{-\epsilon_m}{0.172}\right), \quad \dots (21a)$$

$$B = B_0 + B_1(\chi) + B_2(\chi)^2, \quad \dots (21b)$$

for krypton as

$$A = A_0 + A_1 \exp\left(\frac{-\epsilon_m}{0.283}\right) + A_2 \exp\left(\frac{-\epsilon_m}{2.79}\right) \quad \dots (22a)$$

$$B = B_0 + B_1(\chi) + B_2(\chi)^2, \quad \dots (22b)$$

for xenon as

$$A = A_0 + A_1 \exp[-Ln\{(\epsilon_m/0.578)/2A_2^2\}], \quad \dots (23a)$$

$$B = B_0 \cdot \exp\left(\frac{-T_e}{0.104}\right) + B_1(\chi) + B_2(\chi). \quad \dots (23b)$$

For reference, the fitted curves for ESEC given by continuous line for the maximum energy  $\epsilon_m = 1$  eV of the emitted electrons in argon, krypton and xenon, are shown in Figs. 4, 5 and 6, respectively. Now using Eq. (20) along with Eq. (21) for argon, with Eq. (22) for krypton, and

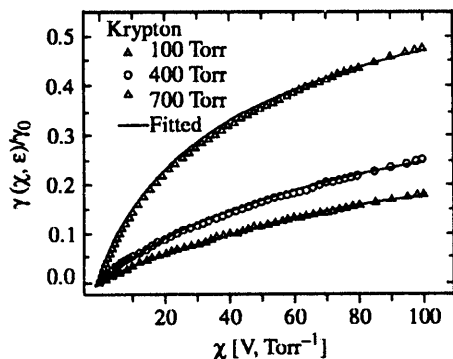


Fig. 5. Estimation and fitting of ESEC for  $\epsilon_m = 1$  eV in Kr.

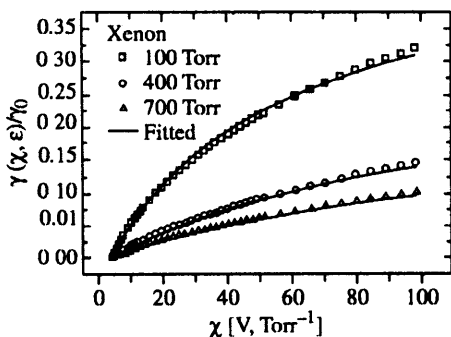


Fig. 6. Estimation and fitting of ESEC For  $\epsilon_m = 1$  eV in Xe.

with Eq. (23) for xenon by introducing the pressure dependence coefficients of  $A$  and  $B$  from Table IV for argon, Table V for krypton, and Table VI for xenon, respectively, one can easily fit  $\bar{\gamma}(\epsilon_m, \chi)/\gamma_0$  to any  $\epsilon_m$  value from 0.2–5 eV for argon, from 0.2–5 eV for krypton, and from 0.1–2 eV for xenon, respectively, for the pressures mentioned in the corresponding tables.

Table 4 : Coefficients of  $A$  and  $B$  for Ar-W.

$p$ [Torr]	$A_0$	$A_1$	$A_2$	$B_0$	$B_1$	$B_2$
100	3.88E-3	4.65E-2	8.27E-1	2.620	1.411	-0.103
200	1.46E-2	1.74E-2	4.88E-1	2.684	2.303	-0.170
300	1.26E-2	1.40E-2	3.40E-1	2.745	3.052	-0.227
400	1.14E-2	1.22E-2	2.63E-1	2.802	3.722	-0.277
500	1.07E-2	1.11E-2	2.17E-1	2.855	4.336	-0.322
600	1.01E-2	1.04E-2	1.85E-1	2.905	4.912	-0.364
700	9.61E-3	9.77E-3	1.62E-1	2.952	5.456	-0.404

Table 5 : Coefficients of  $A$  and  $B$  for Kr-W.

$p$ [Torr]	$A_0$	$A_1$	$A_2$	$B_0$	$B_1$	$B_2$
100	1.31E-2	7.06E-1	3.64E-2	1.928	1.227	-0.074
200	1.11E-2	3.82E-1	2.28E-2	1.826	1.979	-0.121
300	1.00E-2	2.68E-1	1.81E-2	1.741	2.614	-0.160
400	9.29E-3	2.08E-1	1.57E-2	1.666	3.182	-0.195
500	8.79E-3	1.72E-1	1.41E-2	1.598	3.702	-0.226
600	8.41E-3	1.48E-1	1.31E-2	1.535	4.190	-0.255
700	8.11E-3	1.30E-1	1.22E-2	1.476	4.649	-0.282

Table 6 : Coefficients of A and B for Xe-W.

$p$ [Torr]	$A_0$	$A_1$	$A_2$	$B_0$	$B_1$	$B_2$
100	1.32E-2	0.600	4.10E-2	19.09	2.37	1.91
200	1.07E-2	0.634	2.47E-2	30.84	2.39	3.09
300	9.57E-3	0.655	1.90E-2	40.98	2.39	4.10
400	8.90E-3	0.670	1.59E-2	50.24	2.37	5.01
500	8.44E-3	0.681	1.40E-2	58.89	2.35	5.87
600	8.09E-3	0.689	1.27E-2	67.13	2.32	6.68
700	7.83E-3	0.686	1.17E-2	75.02	2.28	7.45

**RESULTS AND DISCUSSION :** For electropositive plasmas, the probe current is comprising of electron and ion currents, and is given by

$$I_p = I_e - I_i \quad \dots (24)$$

where  $I_p$ ,  $I_i$  and  $I_e$  are the probe, ion and electron currents, respectively. In high pressure high density plasmas, under the influence of secondary electron emission, the equation for probe current should be modified and can be written [1] as

$$I_p = I_e - I_i - I_{em} \quad \dots (25)$$

where  $I_{em}$  is the secondary electron emission current. Under the influence of metastable atom fluxes to the probe, the secondary electron emission current from the probe is given [10] as

$$I_{em} = \frac{en_m A_p \gamma}{4} \sqrt{\frac{kT_m}{2\pi m_a}} \quad \dots (26)$$

where  $n_m$ ,  $T_m$ , and  $m_a$  are the concentration, temperature and mass of the metastable atoms, respectively and  $A_p$  is the surface area of the probe. By knowing  $n_m$ ,  $T_m$  and  $m_a$ , and introducing the equation relevant to the gas component used for  $\gamma$ , one can easily be employed Eq. (25) for probe data simulation [1] in order to determine plasma parameters in certain atmospheric pressure plasma conditions.

**SUMMARY :** A kinetic model has been used to estimate effective secondary electron emission coefficients for tungsten in noble gases. Algebraic equations are derived using the estimated emission coefficients and presented in a form suitable for the estimation of secondary electron emission current for the analyses of probe data measured in atmospheric pressure plasmas. Finally, Eq. (25) can be used to determine plasma parameters under the proper discharge conditions at atmospheric pressure. Work is going on to extend this kinetic model for molybdenum and silver also. Work is going on to extend the kinetic model for molybdenum and silver also.

## REFERENCES :

1. Talukder, M.R., Korzec, D. and Kando, M., *J. Appl. Phys.* **91**, 9529 (2002).
2. Korzec, D., Talukder, M.R., and Kando, M., *Science and Tech. Adv. Mat.* (Elsevier) **2/3-4**, 595 (2001).
3. Uytendoeven, W., and Harrington, M.C., *Phys. Rev.* **36**, 709 (1930).
4. MacLennan, D.A., *Phys. Rev.* **148**, 218 (1966).
5. Kenty, C., *Phys. Rev.* **43**, 181 (1933).
6. Molnar, J.P., *Phys. Rev.* **83**, 940 (1951).
7. Mamun, A.A., and Shukla, P.K., *Phys. Plasmas* **10**, 4188 (2003).
8. Mamun, A.A. and Shukla, P.K., *Phys. Plasmas* **10**, (1518) (2003).
9. Shukla, P.K. and Mamun, A.A., *Introduction to Dusty Plasma Physics* Institute of Physics, Bristol, pp. 20-150 (2002).
10. Kagan, M. Yu. and Perel, V.I., *Sov. Phys. : Uspekhi* **6**, 767 (1964).
11. Theobald, J.K., *J. Appl. Phys.* **24**, 123 (1953).
12. Varney, R.N., *Phys. Rev.* **157**, 116 (1967).
13. Nagorny, R.N., and Drallos, P.K., *Plasma Sources Sci. Technol.* **6**, 212 (1997).
14. Hagstrum, H.D., *Phys. Rev.* **96**, 325 (1954).
15. Cazalilla, M.A., Lorente, M., Muino, R.D., Gauyacq, J.P., Billy, D.T. and Echenique, P.M., *Phys. Rev. B.* **58**, 991 (1998-II).